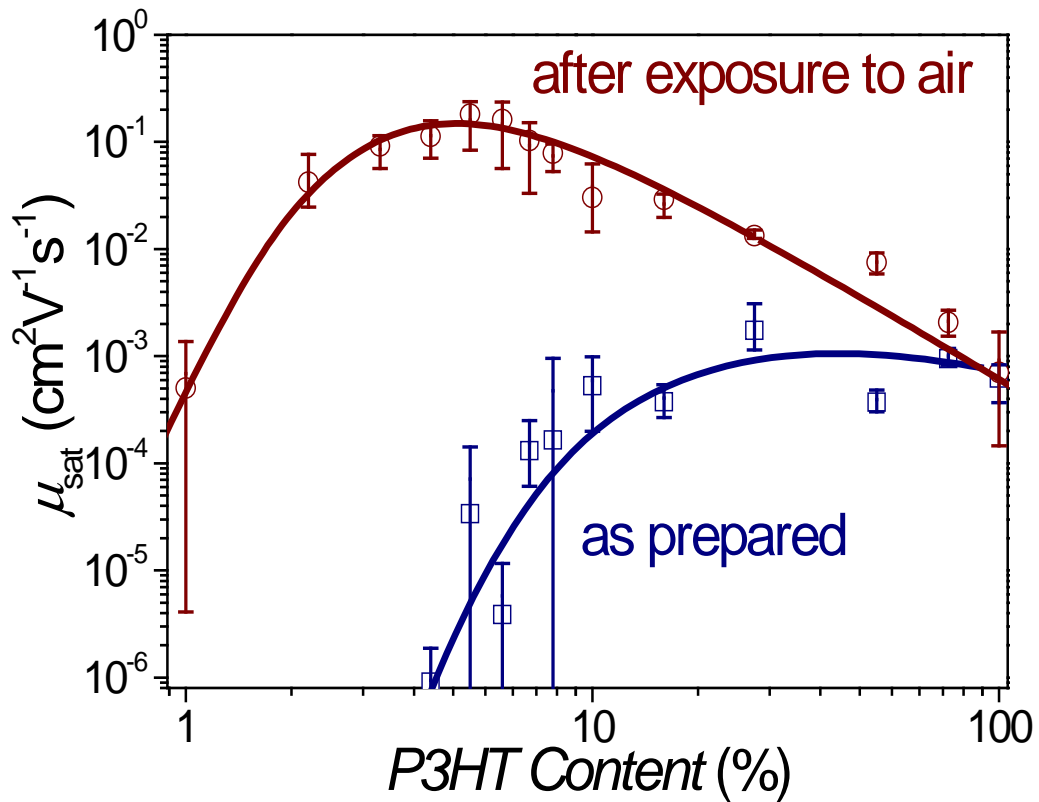
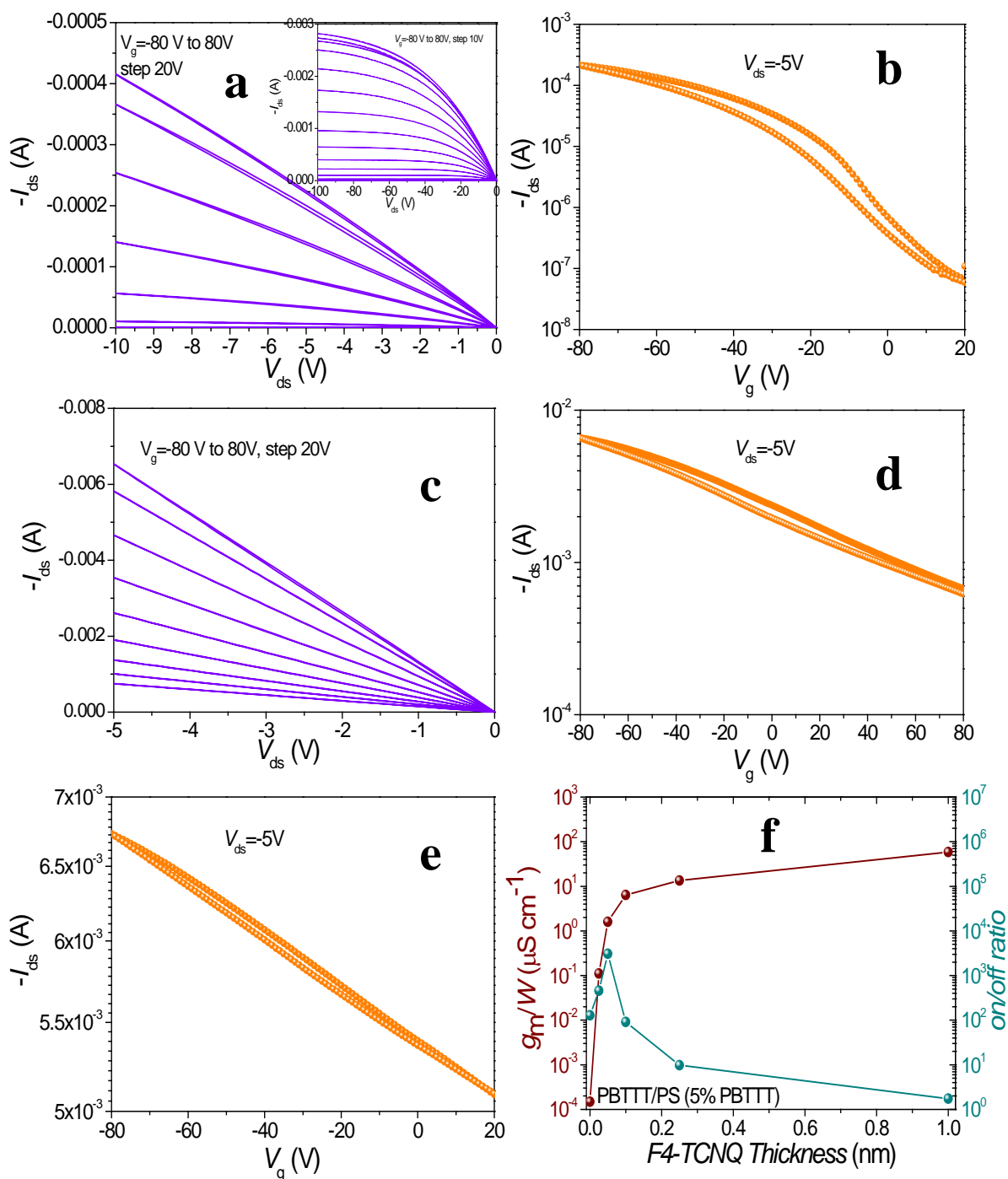


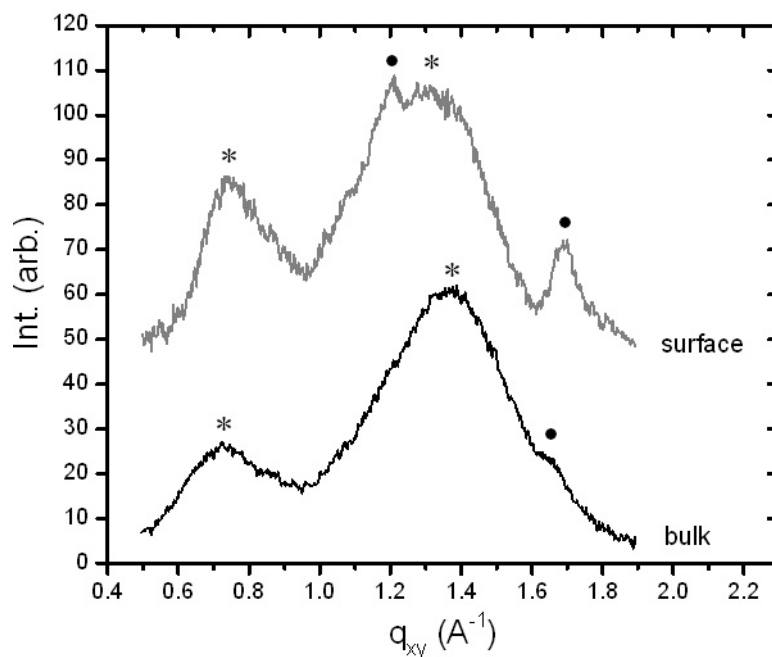
Supplementary Figure S1. In-situ evolution of output characteristics of P3HT/PS (5% P3HT). (a) As prepared. (b) and (c), After 33min and 1143 min in N_2 atmosphere ($O_2 \sim 1$ ppm and $H_2O \sim 1$ ppm), respectively.



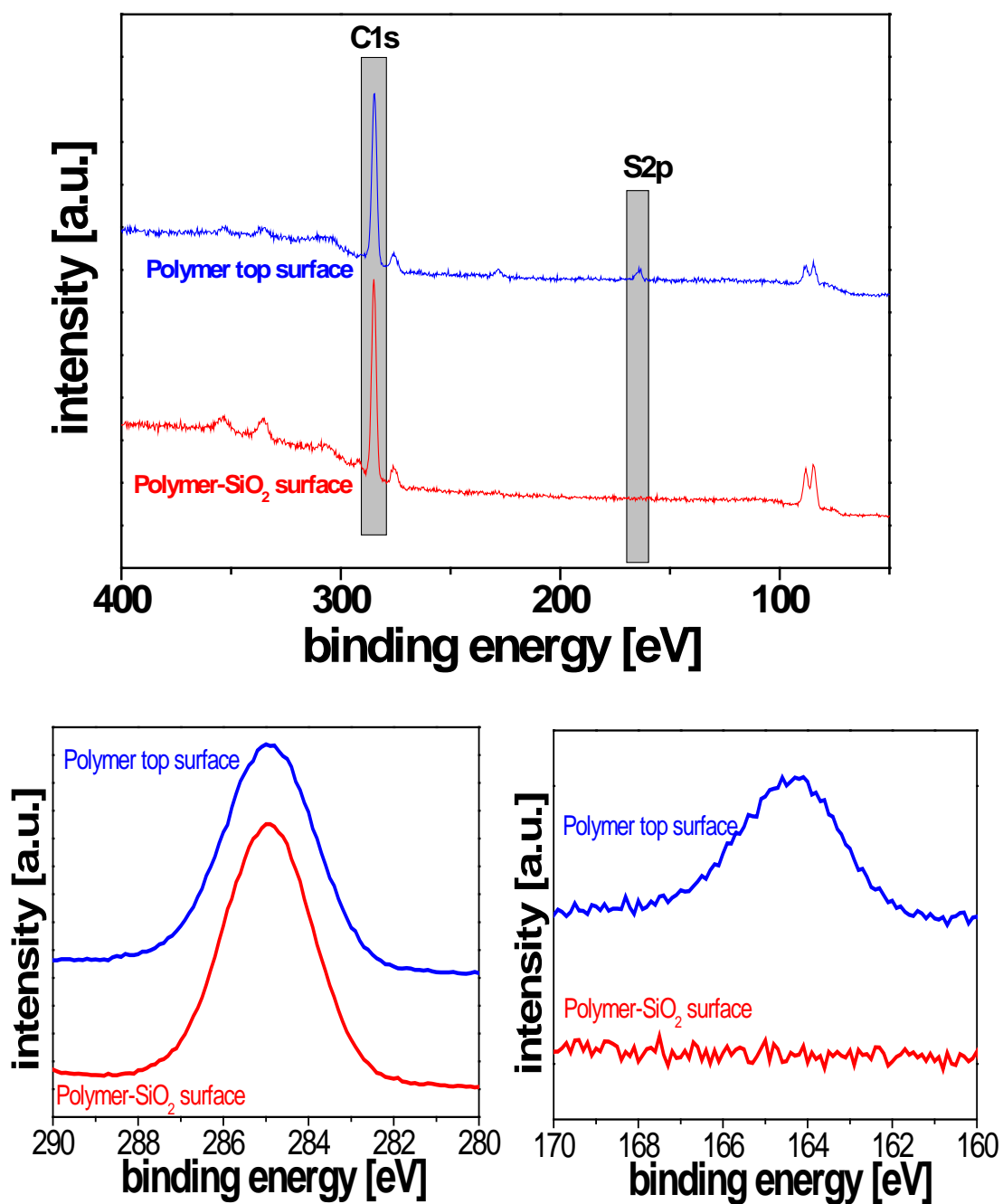
Supplementary Figure S2. The role of P3HT: PS blend ratio. Dependence of μ_{sat} ($V_{\text{ds}} = -100$ V) on the P3HT: PS blend ratio before and after exposure to air for 1 h. Error bar is from more than three devices.



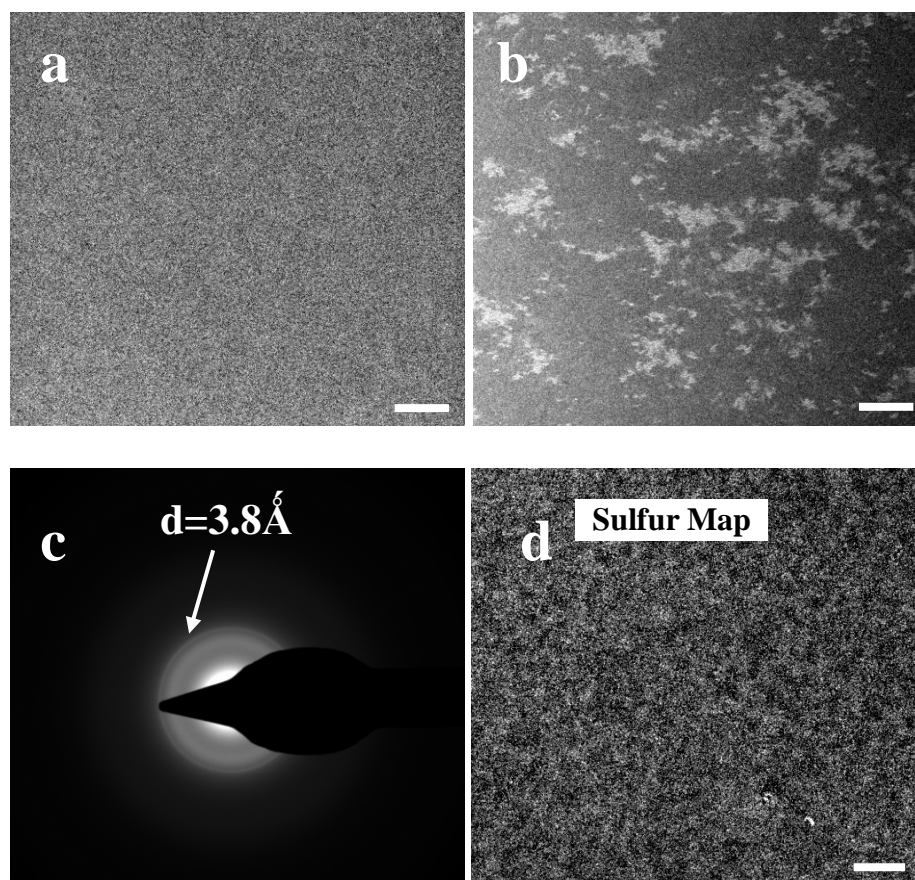
Supplementary Figure S3. OFET characteristics of a PBTTT/PS (5% PBTTT) blend doped by F4-TCNQ with different thickness. (a and b), output characteristics (inset, a larger scale) and transfer characteristics. Dopant, 0.05nm F4-TCNQ ($W = 2.8$ cm). (c) and (d) 0.25 nm F4-TCNQ ($W = 4.3$ cm). (e) 1 nm F4-TCNQ ($W = 0.25$ cm). (f) dependence of normalized transconductance g_m/W and the on/off ratio of PBTTT/PS (5% PBTTT) blend on thickness of the F4-TCNQ.



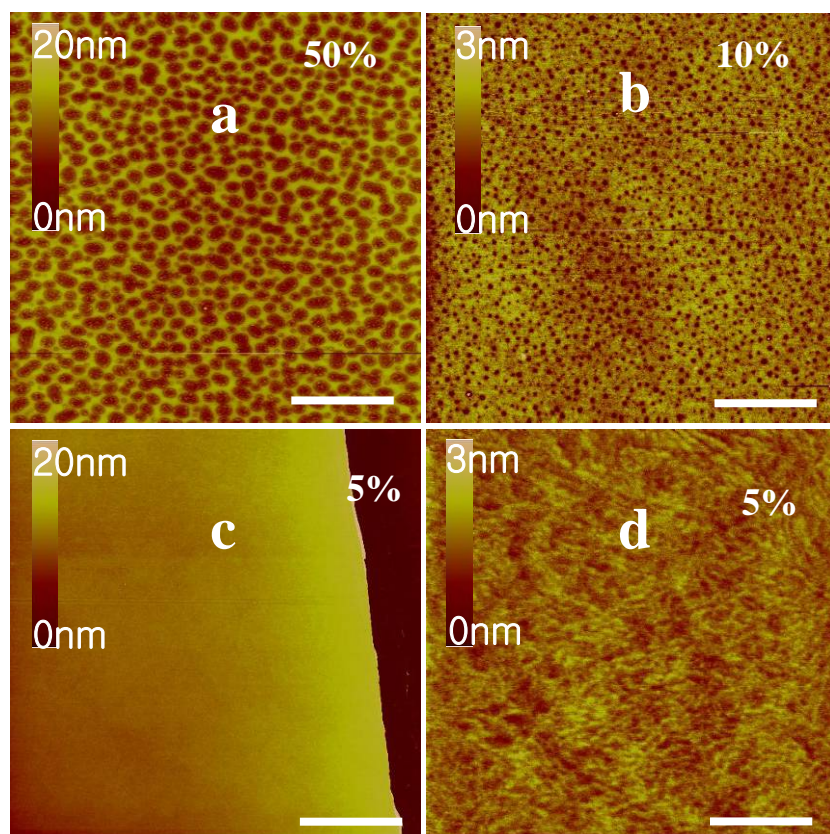
Supplementary Figure S4. In-plane grazing incidence diffraction scans for P3HT/PS (5% P3HT) film. Polystyrene (stars) and P3HT (dots) peaks are indicated and display an enhancement of P3HT in the near-surface region. Incident angles were chosen such that the "surface" measurement probes mainly the top ~10 nm while the "bulk" scan probes the entire film.



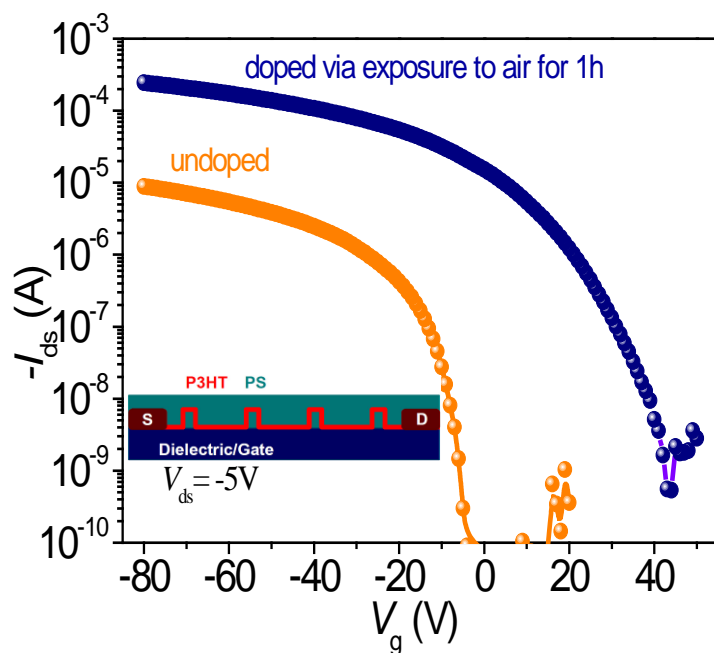
Supplementary Figure S5. XPS spectra of P3HT/PS (5% P3HT). The films were directly peeled-off from OFET substrates with untreated SiO₂ and then transferred onto conducting ITO substrates.



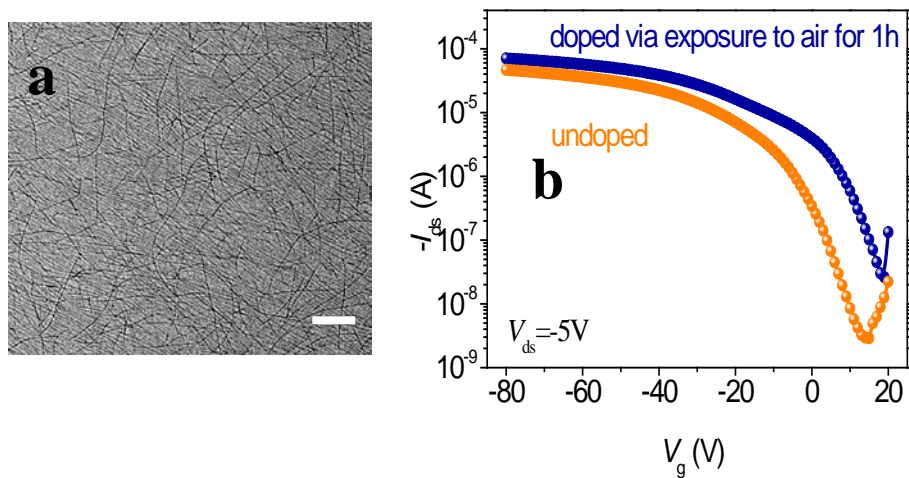
Supplementary Figure S6. TEM of P3HT/PS (5% P3HT) blends. (a and b), Bright-field (a) and dark-field (b) micrographs which show P3HT forms short crystals within PS matrix. (c) Selected-area electron diffraction where a diffraction ring with d -space 3.8 \AA can be identified, according to pi-pi packing distance. (d) Sulfur-map, where brighter area represents higher sulfur content. Scale bars in (a), (b) and (d) represent 500 nm.



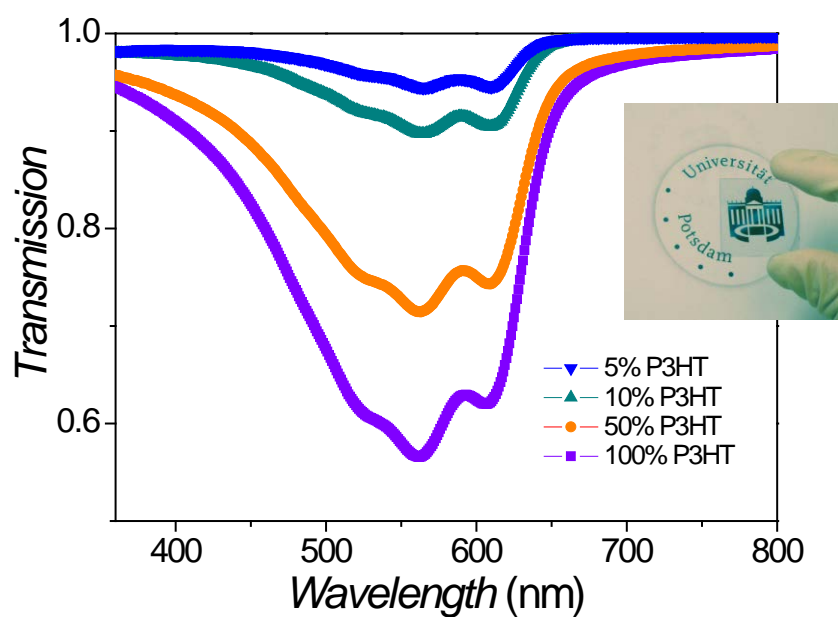
Supplementary Figure S7. AFM topography of P3HT/PS blends. The P3HT contents are denoted in the respective images. (a), (b) and (c) Scale bars, 5 μm. (d) Scale bar, 500 nm.



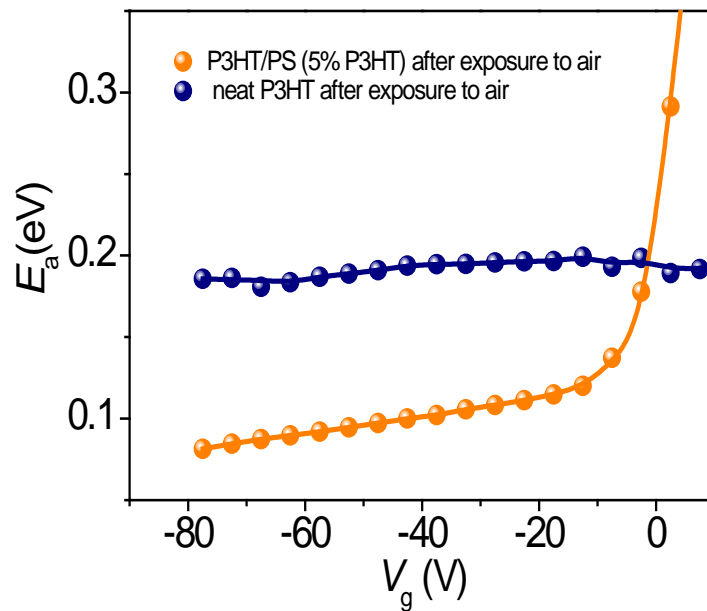
Supplementary Figure S8. Doping behavior of P3HT/PS (5% P3HT) film with an inverted morphology. The film was spincoated on SiO_2 , and then floated onto deionized water surface. We use HMDS/ SiO_2 with Au source/drain electrodes to pick up the film from the backside. The device was then kept in vacuum to remove versatile species (denoted by undoped device). For the doping, the device was exposure directly to air for 1h.



Supplementary Figure S9. Doping behavior of P3BT/PS (5% P3BT) film with long P3BT fiber. **a**, Bright-field TEM, showing P3BT forms fiber-like crystals longer than 1 μm . Scale bar, 500 nm. **b**, Transfer curves of P3BT/PS (5% P3BT) film before and after exposure to air. P3BT/PS (5% P3BT) film was spincoated at 22 $^{\circ}\text{C}$. For the doping behavior of P3BT/PS (5% P3BT) with short fiber, see Figure 2d in the main text.



Supplementary Figure S10. UV-Vis transmission spectrum of spincoated P3HT/PS blend film with different P3HT contents. Inset: a photograph of a spincoated P3HT/PS (5% P3HT) blend film on a glass substrate.



Supplementary Figure S11. Dependence of the activation energy E_a on V_g for neat P3HT and a P3HT/PS (5% P3HT) blend after exposure to air for 1h. E_a was obtained from the temperature dependence of μ_{sat} according to the Arrhenius equation $\mu_{\text{sat}} = \mu_0 \exp(-E_a/kT)$. A liquid N_2 -cooled silver stage (Linkam THMS 600, UK) was used for temperature control.